RSC Advances

PAPER

View Article Online
View Journal | View Issue

Cite this: *RSC Adv.*, 2026, **16**, 20184

Study on key technologies for resource recovery and high-value transformation of main charge in decommissioned explosive tear gas grenades

Xing Fang, †[a] Dandan Liu,†[a] Hualei Yang,[a] Xubo Shen,[b] Xianjun Xie,[a] Zhenhui Li,[a] Tongmei Hu,[a] Zhangyan Hu,*[a] Yongyang Mao*[a] and Zhihao Yi *[a]

To enable the sustainable and harmless treatment of decommissioned explosive tear gas grenades (DTGG), a holistic resource-oriented strategy was developed, which prioritizes the effective recovery of *ortho*-chlorobenzylidene malononitrile (CS) and its transformation into value-added chemical products. Through a systematically developed separation process, CS and RDX were recovered with exceptional efficiency and high purity. The average recovered rate of CS and RDX reached 90.92% and 94.42% respectively, with a purity of more than 98%. The recovered CS was then successfully transformed into 2-(2-chlorophenyl)-benzimidazole (2-CPBZ) *via* an optimized one-pot synthesis achieving an impressive 86.2% yield with 98% purity. Comprehensive characterization and complementary analytical techniques confirmed the structural integrity of both the recovered CS and the synthesized 2-CPBZ. Mechanistic investigations through density functional theory calculations revealed a sophisticated reaction pathway involving sequential nucleophilic addition, acid–base neutralization, nucleophilic substitution, proton transfer, elimination, intramolecular cyclization, and oxidative aromatization. By demonstrating a complete value chain from decommissioned munitions to pharmaceutical intermediates, the research provides both fundamental insights and practical methodologies for green chemical transformation of hazardous materials, opening new avenues for environmentally responsible disposal and resource utilization in defense and security sectors.

Received 23rd February 2026
Accepted 2nd April 2026

DOI: 10.1039/d6ra01583b

rsc.li/rsc-advances

1 Introduction

Although the Chemical Weapons Convention (CWC) prohibits the use of chemical weapons in warfare, it explicitly exempts Riot Control Agents (RCAs) that can rapidly induce sensory irritation or cause transient incapacitation. This specific exemption has led to their widespread adoption for domestic law enforcement and public order maintenance worldwide.[1]

As the most common form of RCAs in global use,[2] tear gas grenades—particularly the widely deployed explosive type CS variant[3]—are characterized by their composition of the riot control agent CS (structure in Fig. S1), the explosive compound cyclotrimethylenetrinitramine (RDX, structure in Fig. S1), the binding agent polyvinyl chloride (PVC), and the plasticizer dibutyl phthalate (DBP).[4] The extensive accumulation of these grenades in warehouses worldwide has resulted in a considerable oversupply. This stockpiling creates serious risks of component leakage, endangering both warehouse personnel and the surrounding environment.

Although incineration and chemical neutralization are the two conventional used technologies for destroying decommissioned tear gas grenades, both are plagued by serious drawbacks.[5–8] The high-temperature oxidative process of incineration risks causing a deflagration-to-detonation transition (DDT) because of the explosive RDX,[9,10] and it generates environmentally hazardous by-products like dioxins.[11] Meanwhile, chemical neutralization which breaks down toxic molecules through specific reactions, suffers from high operational costs and the production of considerable secondary pollutants.[12,13] Therefore, in order to achieve harmless treatment and reduction control of hazardous chemicals,[14] developing environmentally benign and safe disposal technologies is imperative to address the stockpiles of surplus tear gas grenades.

The disposal of tear gas grenades represents an opportunity for resource recovery, given the significant utility of their core components. RDX is a militarily significant explosive with 1.5 times the detonation force of TNT, while CS functions both as a riot control agent and a pharmaceutical synthesis intermediate.[15–17] Solvent extraction technology, recognized for its efficiency and operational simplicity, can be effectively applied to separate and recover these valuable substances.[18,19]

[a]*State Key Laboratory of Chemistry for NBC Hazards Protection, Beijing 102205, China. E-mail: 358032761@qq.com; 8011mao@163.com; 344383569@qq.com; Tel: +(86)18510358993*

[b]*Huazhong University of Science and Technology, Wuhan 430074, China*

† These authors contributed equally to this work.

Adopting such a recycling strategy not only mitigates the environmental impact of destructive methods but also provides a cost-effective source of high-value materials, demonstrating a clear advantage over conventional disposal. Currently, the concept of resource recycling has garnered increasing attention across various industries. For instance, a study by Butturi *et al.* on sustainability-oriented innovation and waste recovery in the textile industry exemplifies the growing emphasis on circular economy principles.[20]

More significantly, the rationale for recycling CS is substantially reinforced by its utility as a versatile chemical building block. Structurally characterized as an arylidene malononitrile, CS possesses reactive functional groups including cyano groups and a carbon–carbon double bond that are amenable to various upgrade pathways. These functional moieties enable advanced valorization pathways such as cyclopropanation and Michael addition,[21,22] effectively converting the reclaimed CS into higher-value chemical products.

The malononitrile functionality can undergo cyclization with *ortho*-phenylenediamine (OPD) to form benzimidazole derivatives, demonstrating a practical route for converting decommissioned CS into valuable synthetic intermediates and effectively transforming a waste stream into a useful resource.[23,24] The benzylidenemalononitrile in CS can react with *o*-phenylenediamine or its derivatives to form benzimidazole derivatives. For example, Jafari-Chermahini *et al.* applied the benzylidenemalononitrile and *o*-phenylenediamine for preparing the arylbenzimidazoles where $SnFe_2O_4$ was used as a catalyst to enhance the yield.[25]

Alternatively, the electrophilic α,β-unsaturated system in CS readily participates in Michael addition with nucleophiles such as the amino group of *o*-phenylenediamine, affording a β-aminonitrile intermediate. Subsequent intramolecular nucleophilic substitution under acidic or basic conditions constructs the imidazole ring, and oxidative aromatization (or spontaneous dehydration) finalizes the formation of the benzimidazole derivative.

Transforming CS into benzimidazole derivatives unlocks access to a privileged scaffold in medicinal science. Benzimidazole is an indispensable heterocycle in novel drug development, where its distinct structure underlies a broad spectrum of biological activities, such as antiviral, antidiabetic, anticancer, and antitubercular effects.[26–28] In anticancer therapy specifically, benzimidazole-based compounds act through multifaceted mechanisms, including inhibiting tubulin polymerization, modulating kinase activity, and interacting with DNA or apoptosis-related proteins.[29,30] The core structure is already validated in the clinic by drugs like nocodazole, bendamustine, and dovitinib.[31,32] This established and high-value application landscape validates the strategic value of repurposing CS into such pharmacologically significant molecules.

Confronting the dual challenges of safely disposing of stockpiled, expired explosive tear gas grenades and the inherent limitations of conventional destruction methods, this study pioneers an integrated "recycle-and-transformation" strategy. Moving beyond mere destruction, a practical pathway for the separation and recovery of the valuable component CS and RDX was established. Moreover, the direct conversion of the recovered CS into pharmacologically relevant benzimidazole derivatives was achieved, substantially increasing its added value. The optimal process conditions were identified, and all outputs were validated using a suite of analytical techniques (SEM, FTIR, NMR, MS). Our approach transforms the problem of grenade disposal into an opportunity for resource recovery, establishing a sustainable and economically attractive alternative to traditional methods.

2 Materials and methods

2.1 Materials and characterization

Detailed information about all materials and characterizations used in this study were provided in the SI.

2.2 Pre-processing of the decommissioned explosive tear gas grenades

The internal charge columns were manually retrieved from the decommissioned grenades. These columns were then treated with acetone at a mass-to-volume ratio of 1 : 10 (g mL^{-1}) to induce swelling and break their compact morphology, thereby facilitating subsequent separation. The treated mixture was passed through an 8-mesh sieve, and the retained solids were air-dried to produce the main charge particles. These particles constituted the target material for all downstream recycling and valorization experiments.

2.3 Separation and purification of the CS and RDX components

To separate CS and RDX from the preprocessed main charge particles, several extraction techniques, including Soxhlet, ultrasonic, and heated stirring, were evaluated. The detailed extraction steps using different methods were provided in SI. The typical protocol was as follows. Firstly, 10 g of the main charge particles were extracted with a 350 mL of methanol under heated stirring at 55 °C in a water bath (HWCL-3, China). The mixture was then filtered. The retained solid was dried and weighed, while the methanol in the filtrate was recovered by rotary evaporation (RE-2000B, China). Next, chloroform was added to the distillation residue to dissolve the CS. After suction filtration, the solid was dried (DHG-9055A, Shanghai) and weighed as crude RDX. The chloroform in the filtrate was evaporated, and the residue was treated with ethanol. This ethanol solution was stirred and then refrigerated at ~5 °C for 1 hour to crystallize the CS. The crystals were collected by filtration, dried, and weighed. All experimental groups were conducted in parallel, and the reported data represent the average values.

2.4 Safety precautions

The main charge is weighed using a copper spoon to avoid static electricity generated by friction. The swelling treatment was performed on a laboratory scale (10 g per batch) at room temperature (20–25 °C) in a well-ventilated fume hood equipped with spark-proof electrical equipment. The chemist wore nitrile

gloves, a lab coat, safety goggles, a face shield, and an anti-static lab coat with grounding to prevent electrostatic discharge during handling.

Purified CS was stored in amber glass vials under nitrogen atmosphere at 4 °C, sealed with PTFE-lined caps to prevent moisture absorption and degradation. Recovered RDX was stored in anti-static polyethylene bottles with grounding, placed in a dedicated explosive storage cabinet at room temperature, away from heat sources and impact, with clear hazard labeling affixed to the containers.

2.5 Synthesis of 2-(2-chlorophenyl)benzimidazole from recovered CS

2.5.1 Synthesis of the CS sulfonate adduct. The CS sulfonate adduct was obtained by reacting CS with sodium hydrogen sulfite ($NaHSO_3$) in an aqueous solution under stirring at room temperature. Typically, deionized water (25 mL) was placed in a 250 mL round-bottom flask. With constant stirring, sodium hydrogen sulfite (50 mmol) was added, followed by the portion-wise addition of CS (50 mmol). The suspension was stirred at room temperature (15–25 °C) for 6 h. The reaction was considered complete when the solid material had fully dissolved with TLC analysis confirming the quantitative consumption of CS. The resulting aqueous solution, containing approximately 50 mmol of the CS sulfonate adduct, was used directly in the subsequent cyclization step.

2.5.2 Preparation of *o*-phenylenediamine monohydrochloride. *o*-Phenylenediamine monohydrochloride was synthesized by reacting *o*-phenylenediamine with concentrated hydrochloric acid in ethanol under stirring at room temperature. Briefly, OPD (75 mmol) was dissolved in absolute ethanol (25 mL) in a 250 mL round-bottom flask under stirring. The hydrochloric acid (75 mmol) was added dropwise over 30 min at room temperature. Then, the mixture was stirred for 2 h to yield *o*-phenylenediamine monohydrochloride.

2.5.3 Synthesis of 2-(2-chlorophenyl)benzimidazole. 2-(2-Chlorophenyl)benzimidazole (2-CPBZ) was synthesized using the *o*-phenylenediamine monohydrochloride mixture (75 mmol) and the CS adduct solution (50 mmol). The crude *o*-phenylenediamine monohydrochloride mixture (75 mmol), serving as both a reactant and an acid catalyst, was placed in the reaction flask. The aqueous CS adduct (50 mmol) was added dropwise at room temperature under stirring. The reaction was allowed to proceed at room temperature for 4 h. Sodium formate (125 mmol) was then added, and after 30 minutes of stirring, the mixture was heated to 70 °C and held for 3 h. A prominent precipitate formed during the heating stage. After TLC confirmed the full consumption of the CS adduct, the mixture was cooled from 70 °C to room temperature in approximately 1 hour. The product was collected by filtration, subjected to a standard wash cycle, and vacuum-dried. All experiments were conducted in triplicate, and the results are presented as mean values.

2.6 Density functional theory (DFT) calculation details

DFT calculation is an important tool for explaining micro reaction mechanisms, elucidating intermolecular interactions, and activation energy transitions.[33] The calculation details about the transformation of CS are described in SI.

2.7 Detection and calculation methods

2.7.1 Detection of CS and 2-CPBZ. The concentrations of CS and the synthesized product, 2-CPBZ, were quantified using High-Performance Liquid Chromatography (HPLC, Thermo Fisher Scientific TCC-3000SD, America) equipped with an ultraviolet detector. The model of chromatographic column is Acclaim™ 120 (C18, 5 μm). UV detector (Ultimate 3000) is used for analysis.

For CS quantification, the analysis was performed using a mobile phase of acetonitrile and water (60 : 40, v/v) at a flow rate of 1.0 mL min^{-1}. Detection was carried out at 300 nm with an injection volume of 10 μL. A calibration curve was constructed using standard solutions at concentrations of 5, 10, 30, 50, 100, and 200 μg mL^{-1}, and sample concentrations were determined *via* the external standard method.

For 2-CPBZ, the HPLC analysis was performed using a mobile phase comprising 0.1% triethylamine, acetonitrile, and 10 mmol ammonium acetate with 0.1% formic acid (15 : 25 : 60, v/v) at a flow rate of 1.2 mL min^{-1}. Detection wavelength was set at 286 nm with a 10 μL injection volume. A series of standard solutions (10, 20, 50, 70, 100, and 120 μg mL^{-1}) were analyzed to establish the calibration curve *via* the external standard method.

2.7.2 Calculation of yield and purity of CS and 2-CPBZ. The yield of the recovered CS from the main charge was calculated in eqn (1) (eqn (1)), where W_{CS} refers to the yield of CS, (%); M_{CS} represents the mass of the recycled CS, (g); M is the mass of the main charge, (g); A is the certified mass fraction of CS in the main charge. Due to the confidentiality of the product formula, the value of A will not be disclosed to the public.

$$W_{CS} = \frac{M_{CS}}{M \times A} \times 100\% \quad (1)$$

The purity of the recovered CS (Y, %) was determined *via* HPLC analysis of a prepared solution and calculated using eqn (2), where Y represents the purity of CS (%); C is designated for the determined concentration of CS solution (μg mL^{-1}); V is the volume of CS solution (mL) and m is the mass of the weighed CS.

$$Y = \frac{C \times V}{m} \times 10^{-4} \quad (2)$$

The calculation of the purity of the 2-CPBZ (Y, %) was similar with the recovered CS, determined *via* HPLC analysis of a prepared solution.

The yield of 2-CPBZ was calculated by the eqn (3).

$$W = \frac{W_1 \times Y}{M_1} \times 100\% \quad (3)$$

In this equation, W is the yield of 2-CPBZ, %; W_1 represents the mass of the actual production, g; Y stands for the purity of

the synthesized 2-CPBZ, %; M_1 is referred to the mass of the theoretical production, g.

3 Results and discussion

3.1 The recycle of CS from decommissioned explosive tear gas grenades

3.1.1 Determination of the separation and recycling process. Guided by practical considerations of cost and commercial availability, methanol, ethanol, acetone, and chloroform were chosen to investigate the temperature-dependent solubility of CS and RDX (Fig. S1). The detailed analysis was provided in the SI. An efficient separation and recycle process route was designed (Fig. 1). The specific procedure was as follows. Firstly, the main charge particles were extracted with methanol (Fig. S2). Due to the poor solubility of PVC in methanol, it was effectively separated by suction filtration as a solid residue. The filtrate containing CS, RDX, and DBP, was then subjected to reduced-pressure distillation to recycle methanol. The distillation residue was then dissolved in chloroform at room temperature. RDX, which is poorly soluble in chloroform, was isolated as a solid *via* filtration. The filtrate, containing CS and DBP, was subsequently treated by rotary evaporation to recover chloroform. In addition, several alternative solvents to chloroform were also evaluated. As shown in Fig. S3, chloroform proved to be the most suitable solvent for the separation of CS and recovery of RDX under the tested conditions. Finally, the remaining residue (CS and DBP) was treated with cold ethanol under stirring. Based on their differential solubility, DBP dissolved in ethanol, while CS remained as a solid. Filtration was used to separate solid CS, and the ethanol filtrate containing DBP was concentrated to recover both DBP and the solvent.

In comparison with conventional disposal methods, the entire workflow significantly reduces energy consumption and solvent usage through multi-step solvent recycling (methanol, chloroform, and ethanol). It also minimizes secondary pollution and enables the resource recycle of CS, RDX, DBP, and PVC, offering combined environmental and economic benefits.

3.1.2 Optimization of separation and recycling process. To enhance the yield of CS, various separation conditions including extraction methods, material ratios, processing time, temperature gradients, and scaling factors were investigated. By designing single-factor experiments, the separation process parameters were refined and optimized.

Before the heat extraction, the TG-DTA curves of RDX was analyzed in Fig. S4. The thermal decomposition onset temperature is above 200 °C, providing a substantial safety margin for operations at 55–70 °C.

As shown in Fig. 2(a), the heated-stirred extraction method yielded the highest CS recovery rate (90.63%), outperforming Soxhlet (77.49%), ultrasonic (88.60%), and stirred (86.24%) methods. To ensure a fair comparison, all operating parameters were kept constant across the different extraction methods. The solid-to-liquid ratio was fixed at 1 : 35, the extraction time was 30 minutes for all methods, and the temperature was maintained at 55 °C for methods involving heating (except Soxhlet extraction, which was performed at the boiling point of methanol under reflux). The superior performance, attributed to improved mixing uniformity, led to the selection of the heated-stirred method for further process optimization. Given the impact of mixing intensity on extraction efficiency, the stirring speed was systematically optimized. As shown in Fig. S5, 500 rpm was determined to be the optimal condition.

The solid-to-liquid ratio was optimized to equilibrate extraction yield and cost. As depicted in Fig. 2(b), the CS recovery rate remained consistently around 90% across ratios ranging from 1 : 25 to 1 : 40, attributable to the high solubility of CS in methanol. At ratios above 1 : 25, both CS and RDX yields

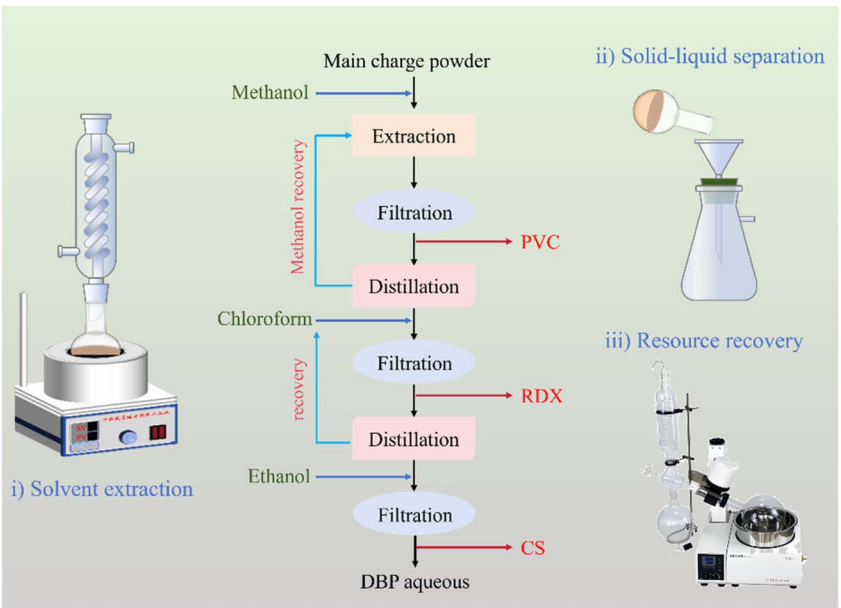

Fig. 1 The separation and recycle process route.

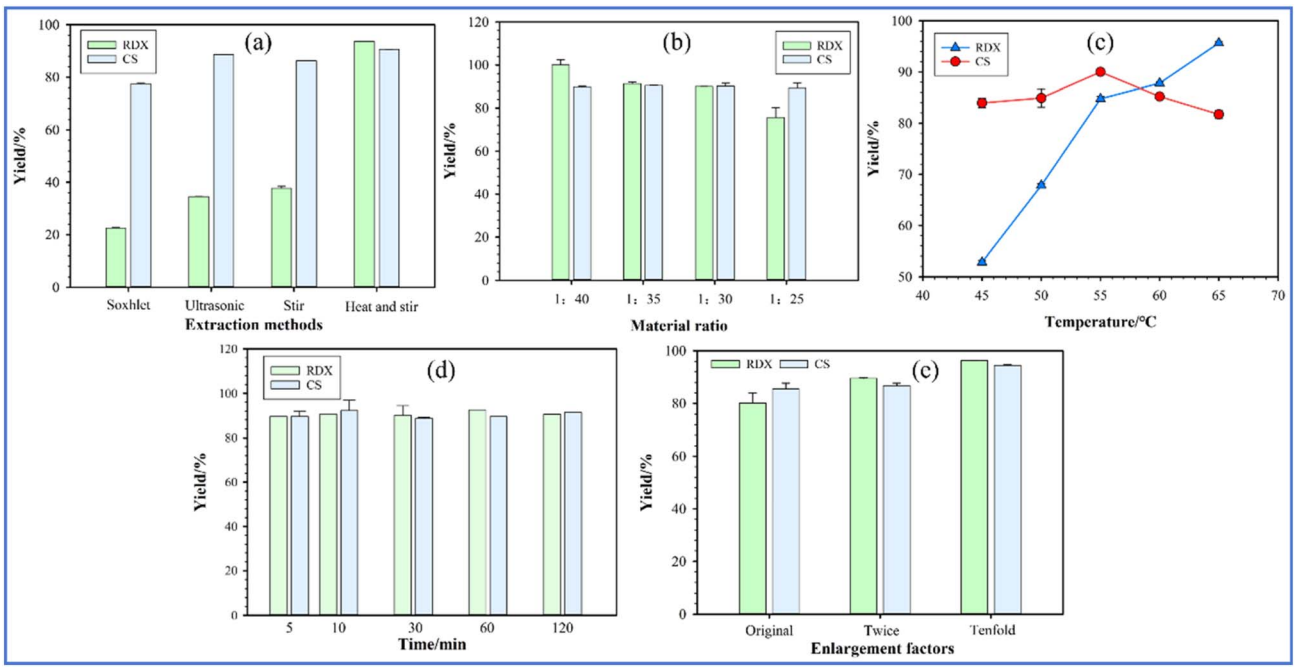

Fig. 2 The yield of CS and RDX affected by different factors (a) extraction methods, (b) material ratio, (c) temperature, (d) time, (e) enlargement factors.

were satisfactorily high (>90% and >80%, respectively). A ratio of 1 : 35 was chosen as the optimal condition, ensuring efficient extraction while maintaining practical reactor operation and process stability.

The effect of the extraction temperature was displayed in Fig. 2(c). As the temperature rose from 45 °C to 55 °C, the CS recovery increased markedly from 83.97% to a maximum of 90.00%. However, a further increase to 60 °C resulted in a decline to 81.75%, likely attributed to the incipient decomposition or side reactions of CS. Therefore, 55 °C was identified as the optimal extraction temperature.

The influence of extraction time is presented in Fig. 2(d). The CS yield rose rapidly to 89.50% within 10 min and stabilized thereafter, reaching a maximum of 92.54%. It indicates that efficient dissolution of CS in this process was achieved within approximately 10 minutes.

To validate the robustness and scalability of the optimized process, laboratory-scale amplification experiments were conducted under the determined optimal conditions. The quantities of the main charge and extracting agent were proportionally increased with scaling factors of 2× and 10×. The cooling time for CS recrystallization was approximately 30 minutes (cooling to 5 °C). As shown in Fig. 2(e), the CS yield exhibited a positive correlation with the scaling factor, increasing significantly from 80.12% at the baseline to 94.48% at the 10× scale. This scale-dependent enhancement in recovery not only confirms the high efficiency and stability of the process across different operational volumes but also verifies its scalability, providing key insights for future industrial application.

3.1.3 Characterization of recycled CS. To confirm that the isolated product was CS and to characterize its physicochemical properties, a series of spectroscopic analyses were performed. The nuclear magnetic resonance (NMR) analyses of the recycled CS sample, including proton (^{1}H NMR) and carbon (^{13}C NMR) spectra, are presented in Fig. 3(a). ^{1}H NMR (400 MHz, $CDCl_3$, TMS, 25 °C) $\delta = 8.27$ (s, 1H), 8.18 (d, $J = 7.9$ Hz, 1H), 7.56 (d, $J =$ 4.2 Hz, 2H), 7.45 (dp, $J = 8.8$, 4.5 Hz, 1H). ^{13}C NMR (101 MHz, $CDCl_3$) δ = 156.11, 136.36, 135.09, 130.73, 129.52, 129.06, 127.82, 113.26, 111.95, 85.76. ^{13}C NMR (151 MHz, DMSO) δ 149.08, 143.21, 134.64, 132.07, 131.63, 131.18, 130.33, 129.97, 127.42, 122.72, 121.67, 119.08, 111.69. All chemical shift (δ) values match those reported in the literature for CS.[34] The mass spectrometry fitting results for the recycled CS were shown in Fig. 3(b). The molecular weight of the tested sample is approximately 188.01, which is close to the theoretical molecular weight of CS (188.61). Together with the NMR results, this confirms that the recovered sample is CS.

From the FTIR results in Fig. 3(c), the recycled sample is highly similar to the certified reference in terms of chemical structure and functional group composition. Characteristic peaks were observed at the following wavenumbers: 3046 cm^{-1} (stretching vibration of unsaturated =C–H bonds); 2934 cm^{-1} (stretching vibration of saturated C–H bonds); 2224 cm^{-1} (stretching vibration of –C≡N groups); 1906 cm^{-1} (stretching vibration of cumulative double bonds); 1578 cm^{-1} (skeletal vibration of the aromatic ring); 1042 cm^{-1} (stretching vibration of C–Cl bonds); Peaks at 1433 cm^{-1}, 1285 cm^{-1}, 1207 cm^{-1}, 1122 cm^{-1}, and 959 cm^{-1} are associated with the stretching vibrations of C–N bonds.[35,36]

The SEM results was displayed in Fig. 3(d). It could be seen that the certified reference exhibited a smooth surface and dense texture, while the recycled CS showed a slightly porous

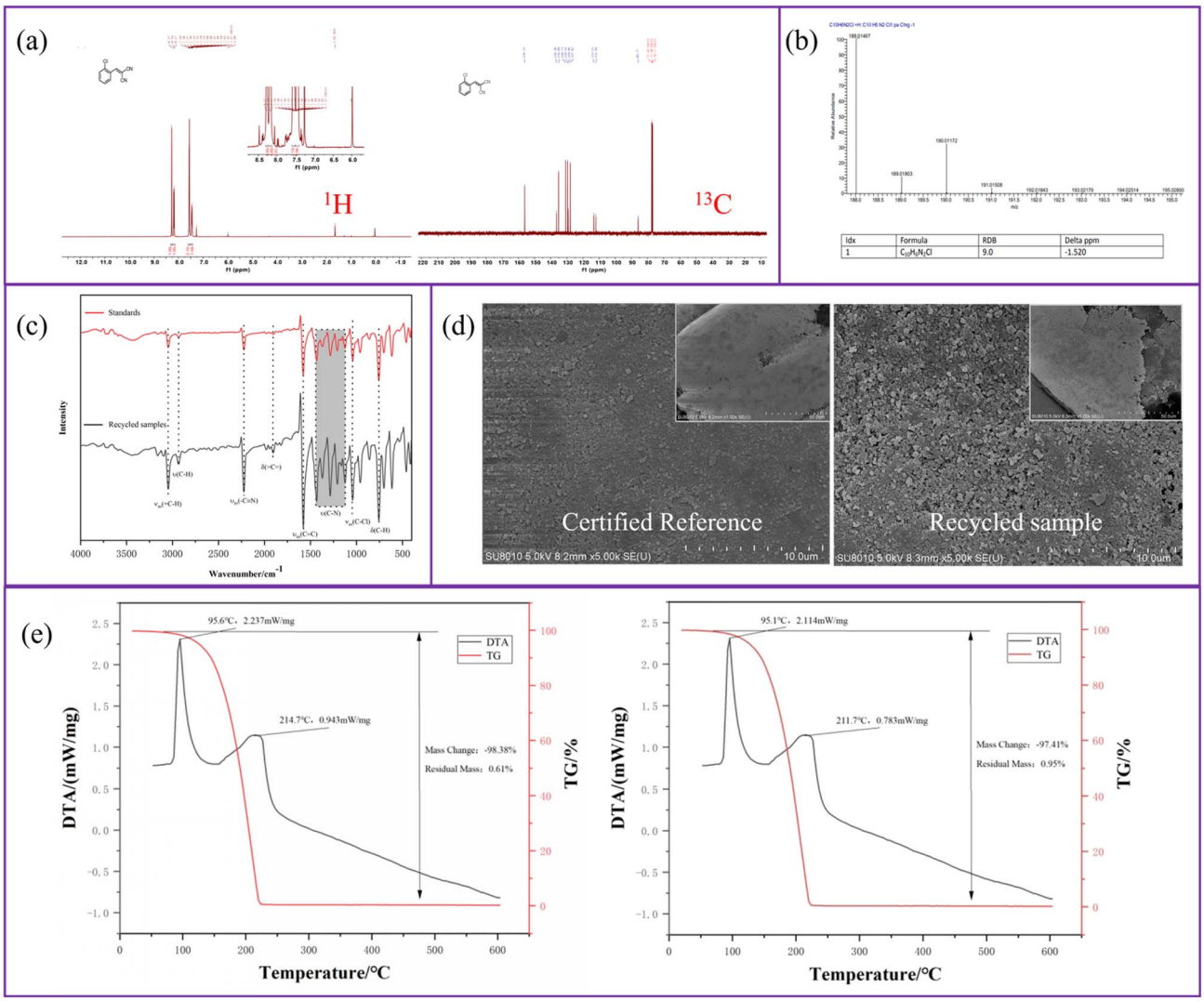

Fig. 3 Various characterizations of CS certified reference and recycled sample (a) NMR, (b) FTIR, (c) MS, (d) SEM, (e) TG-DTA curves.

surface. The SEM images at different magnifications (50.0 μm and 10.0 μm) revealed that both the recycled sample and the certified reference display typical agglomerated microstructures.

As shown in Fig. 3(e), the certified reference exhibited a melting peak at 95.4 °C without mass loss, followed by exothermic decomposition after 212.3 °C accompanied by a sharp mass decline. The mass change was 96.39%, indicating nearly complete decomposition. In comparison, the recycled sample showed a similar thermal behavior with only slight deviations: the melting peak position shifted marginally, and vigorous exothermic decomposition started above 214.7 °C, resulting in a mass loss exceeding 98%. Overall, the thermal behavior of the recycled sample aligns well with that of the certified reference.

The crystal morphology of CS varies with production and crystallization conditions, and its melting behavior correlates with crystal state. Experimental measurements showed that the initial and final melting temperatures of CS samples were concentrated at (94.5 ± 1.0) °C and (96.0 ± 0.5) °C, respectively (Table S1). Both values deviate by less than 2.0 °C from those of the certified reference, demonstrating high consistency in crystal structure.[37] The results are corroborated by TG-DTA and SEM analyses, confirming the crystal structural stability of the recycled CS sample.

In summary, through a combination of spectroscopic, thermal, and morphological characterization techniques, the recycled sample has been conclusively identified as CS with high purity and structural integrity comparable to the certified reference material.

3.1.4 The purity and yield of the recycled CS and RDX. As demonstrated in Fig. S6, the solvent maintained its performance over more than three consecutive reuse cycles, highlighting its excellent economic feasibility. The solvent recovery efficiency remained stable during the first three cycles, with CS and RDX recovery consistently >85% and purity >98%. However, after the fourth cycle, a noticeable decline in RDX recovery was observed (70%), likely due to the decrease of dissolved RDX with the decrease of recycled solvents. Therefore, we recommend

Table 1 The purity and yield of the recycled CS and RDX

Experiments	Yield of CS/%	Purity of CS/%	Yield of RDX/%	Purity of RDX/%
1	93.65	98.30	95.45	97.76
2	90.48	98.60	95.45	98.22
3	90.16	98.10	94.09	98.73
4	92.54	98.81	93.64	97.05
5	90.00	98.77	92.73	98.84
6	90.63	98.83	93.64	99.11
7	88.70	98.24	100	98.82
8	91.90	99.13	95.90	97.45
9	90.00	98.70	88.64	99.06
10	91.10	99.49	94.70	99.57

a maximum of three reuse cycles to ensure consistent separation performance (Fig. S6).

To verify the stability of this process, 10 batches of repeat experiments were conducted under the optimal conditions, with systematically investigation of the variations in the yield and purity of CS across different batches (Table 1). Under the optimal process conditions, the average recycle rate of CS exceed 90%, while its purity was higher than 96%. For RDX, the recycle rate and purity of which was determined to be 94.42% and 98.46, respectively.

These results indicate that the extraction process exhibits excellent reproducibility and operational stability, consistently delivering high-quality CS with uniform performance across multiple batches. In conclusion, the CS separation and recycle process established in this study proves to be both efficient and highly stable. It provides a reliable technical foundation for subsequent valorization of CS and potential industrial-scale application.

3.2 High-value conversion of CS to 2-CPBZ

The reactive sites within the CS molecule provided a unique structural foundation for its resource utilization. The α,β-unsaturated carbon atoms exhibited low electron density due to the strong electron-withdrawing effect of the two conjugated nitrile groups, rendering them susceptible to nucleophilic addition.[38] Although the nitrile group in the molecules shows weak nucleophilicity due to conjugation with the benzene ring, their reactivity could be modulated through protonation or coordination, enabling controllable functional group transformations for multi-step organic synthesis.

Based on the reactivity profile, we proposed a strategy to transform CS into high-value benzimidazole derivatives (*e.g.*, 2-CPBZ). This synthetic route not only completely eliminates the environmental risks associated with scrapped CS, but also achieves waste valorization by transforming a hazardous material into a valuable chemical intermediate.

3.2.1 Establishment of reaction routes and process optimization. The synthesis involving CS and *o*-phenylenediamine is hampered by its reliance on catalysts and high temperature condition, which induces oxidative side reactions at the amine groups and ultimately limits the yield.[39] To address this issue, two key modifications were implemented: (i) *o*-phenylenediamine was protonated to its hydrochloride salt, enhancing its thermal stability and suppressing undesirable oxidation,[40] ensuring that OPD remains available for the desired nucleophilic addition. The protonation of the amino groups reduces their electron-donating ability, making them less susceptible to oxidation and thereby suppressing undesired radical-mediated polymerization. (ii) CS was preactivated by conversion into a sulfonate adduct, thereby reducing the energy barrier for nucleophilic attack and enabling the reaction to proceed under milder conditions.

Then, the "one-pot" reaction of CS sulfonate with OPD facilitates a sequential transformation involving intermolecular nucleophilic substitution, *in situ* neutralization, intramolecular cyclization, and oxidative aromatization.

To establish the optimal protocol for converting CS to 2-CPBZ, a thorough investigation of reaction parameters was undertaken. The effect of temperature was firstly investigated by reacting 25 mmol of the CS sulfonate adduct with 37.5 mmol of OPD for 3 hours. As shown in Fig. S7(a), the yield exhibited a volcano-shaped dependence on temperature. It increased from 61% at 60 °C to over 85% at 70 °C, then declined to 73% at 80 °C. The suboptimal yield at 60 °C is attributed to insufficient thermal energy to overcome the activation barrier for the intramolecular cyclization, compounded by the endothermic nature of the oxidative aromatization, leading to incomplete conversion. At 80 °C, side reactions such as nucleophilic addition between free amino and cyano groups forming benzodiazepine-like byproducts, and oxidation or polymerization of *o*-phenylenediamine complicated purification and reduced the yield.

Varying the amount of OPD revealed that the yield reached a maximum of 86.1% at a 1.5 : 1 molar ratio to the CS sulfonate adducts (Fig. S7(b)), beyond which no further gain was observed. Finally, under optimized conditions (25 mmol CS adduct, 37.5 mmol *o*-phenylenediamine monohydrochloride, 70 °C), the reaction time was varied. As shown in the Fig. S7(c), the yield increased with time and peaked at 86.5% after 3 h. Further extension of the reaction led to a decreased yield and noticeable product darkening, attributable to over-oxidation of the excess amine compounds. Therefore, 3 h was identified as the optimal reaction duration. In conclusion, the optimal conditions for converting CS to 2-CPBZ are established as follows: a molar ratio of 1.5 : 1 for OPD to CS sulfonate adduct, a reaction time of 3 h, and a temperature of 70 °C.

The conversion of CS into 2-CPBZ presents a robust and efficient synthetic route with significant merits. (i) Mild conditions: the Michael addition-cyclization between OPD and CS proceeds at room temperature or with mild heating, requiring no specialized equipment and demonstrating excellent process adaptability. (ii) High selectivity: the intramolecular cyclization selectively forms the benzimidazole ring with minimal side reactions, yielding high-purity product. *o*-Phenylenediamine, an industrial bulk chemical, shows excellent compatibility with CS without risk of violent exothermic reactions.

3.2.2 Characterization of converted 2-CPBZ. To confirm that the product synthesized from CS was the target 2-CPBZ,

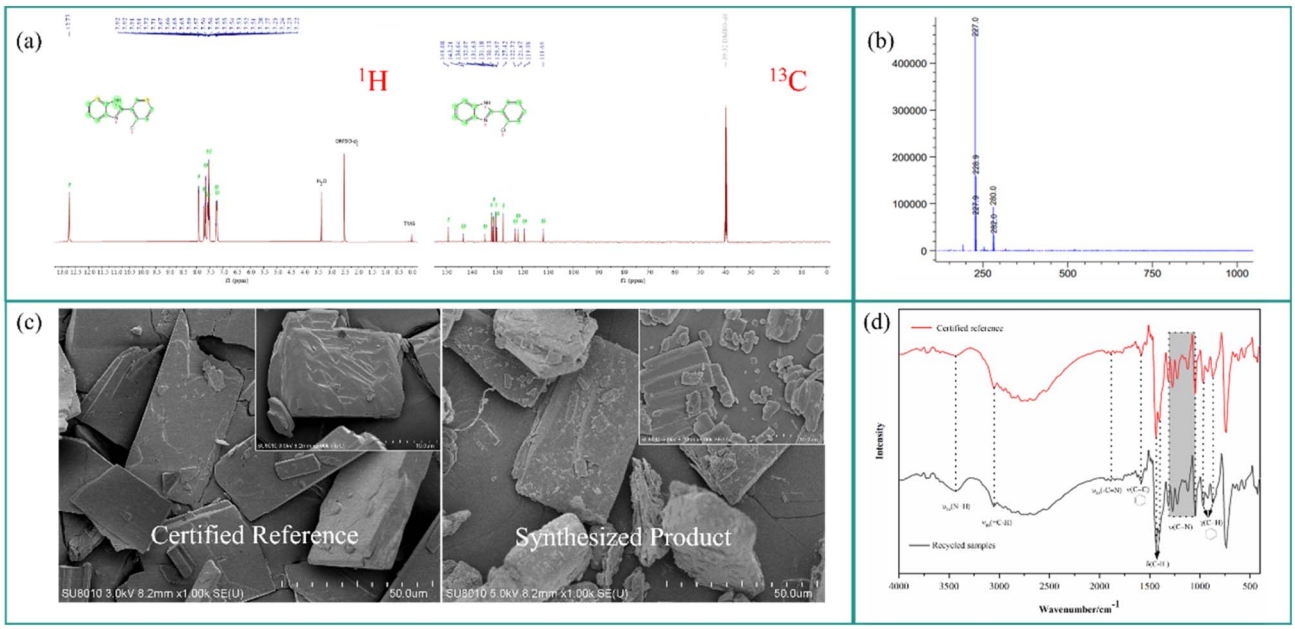

Fig. 4 Various characterization results of 2-CPBZ (a) SEM, (b) FTIR, (c) NMR, (d) MS.

a comprehensive characterization was performed using spectroscopic and morphological techniques.

The molecular structure was firstly confirmed by NMR and MS (Fig. 4(a and b)). The ^{1}H NMR spectrum (600 MHz, DMSO) displayed characteristic signals at δ 12.73 (s, 1H), 7.92 (dd, J = 7.3, 2.1 Hz, 1H), 7.71 (d, J = 7.9 Hz, 1H), 7.67–7.64 (m, 1H), 7.58 (d, J = 7.9 Hz, 1H), 7.57–7.50 (m, 2H), 7.27 (t, J = 7.3 Hz, 1H), and 7.23 (d, J = 7.6 Hz, 1H). The ^{13}C NMR (151 MHz, DMSO) showed characteristic signals at δ 149.08, 143.21, 134.64, 132.07, 131.63, 131.18, 130.33, 129.97, 127.42, 122.72, 121.67, 119.08, 111.69.[41,42] Mass spectrometry revealed a molecular ion peak at m/z 227.0, consistent with the theoretical molecular weight of 2-CPBZ (228.68).

SEM results (Fig. 4(c)) revealed that the CS-synthesized crystals showed inferior surface integrity with increased debris and fractures, crystallized in lamellar structures. The morphological difference is attributed to accelerated crystallization at elevated temperature and mechanical stirring-induced crystal damage during synthesis.

FTIR analysis further corroborated the structural assignment. As shown in Fig. 4(d), the spectrum of the synthesized 2-CPBZ from CS was nearly identical to that of the certified reference. Characteristic absorptions included O–H stretching (3727 cm^{-1}), N–H stretching (3440 cm^{-1}), aromatic C–H stretching (3053 cm^{-1}), C≡N stretching (1889 cm^{-1}), aromatic skeleton vibration (1585 cm^{-1}), and C–N stretching between 1314–1045 cm^{-1},[43] confirming matching functional group composition.

2-CPBZ exhibits consistent thermal behavior regardless of its physical form, with both certified reference and synthesized samples displaying nearly identical melting characteristics. The results of melting point are shown in Table S2.

3.2.3 Mechanism of the transformation. The reaction mechanism for the synthesis of 2-CPBZ from CS and OPD was systematically investigated using DFT calculations, as illustrated in Fig. 5. The transformation proceeds mainly include nucleophilic addition, acid–base neutralization, nucleophilic substitution, proton transfer and elimination, intramolecular nucleophilic cyclization, and oxidative aromatization.

Compound **1** first undergoes a Michael addition reaction with $NaHSO_3$ to form CS sulfonate (compound **2**). The Gibbs free energy change (ΔG) for this process is −11.6 kcal mol^{-1}, indicating that the reaction is spontaneous and exothermic. The lone pair electrons on the sulfur atom of the HSO_3^- nucleophile attack the highly electron-deficient α-carbon of compound **1**, leading to π-bond cleavage and transfer of the negative charge to the β-carbon, forming a carbanion intermediate. This intermediate is subsequently protonated to yield the stable compound **2**. OPD reacts with hydrochloric acid to form the monohydrochloride salt (compound **3**). The sulfonate group in compound **2** then acts as a good leaving group, enabling nucleophilic substitution with the free amino group in compound **3**. DFT calculation indicates that the transition state TS1 for this step has an activation energy (E_a) of 23.1 kcal mol^{-1}, consistent with the experimentally observed requirement for heating. Relaxation of TS1 generates intermediate compound **4**, subsequently undergoing a lower-energy barrier reaction (E_a = 14.6 kcal mol^{-1}) to form compound **5**. And it reacts spontaneously with sodium formate in a neutralization step (ΔG = −4.5 kcal mol^{-1}) to give compound **6**.

Two competing pathways were evaluated for the cyclization of compound **6** to compound **9**. Path A involves intramolecular nucleophilic substitution, where the amino group attacks the α-carbon *via* transition state TS2A (E_a = 33.0 kcal mol^{-1}), leading to direct malononitrile elimination to form compound **9**. In

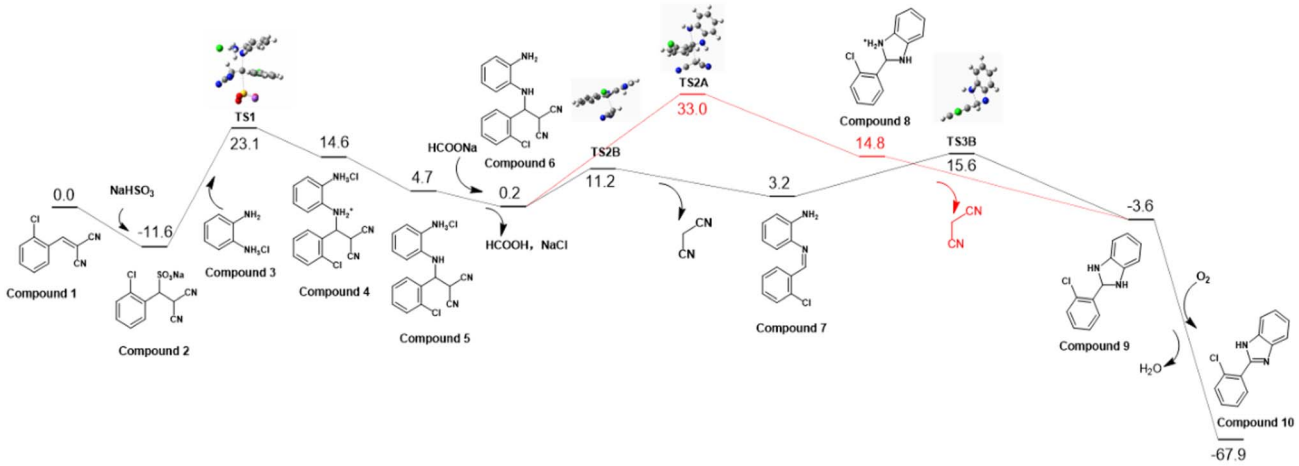

Compound 1：CS
Compound 2：CS sulfonate salt
Compound 3：O-phenylenediamine dihydrochloride
Compound 6：2- [2- (phenylenediamino)] - chlorophenylmalononitrile
Compound 5：2- [2- (phenylenediamino)] - chlorophenylmalononitrile hydrochloride
Compound 7：2-[(2-chlorobenzylidene)amino]aniline
Compound 9：2- (2-chlorophenyl) benzimidazoline
Compound 10：2- (2-chlorophenyl) benzimidazole

Fig. 5 Mechanism of the conversion of CS.

Table 2 The purity and yield of 2-CPBZ

Experiments	1	2	3	4	5	Average	RSD
Yield (%)	85.5	85.7	86.1	86.3	87.0	86.2	0.67%
Purity (%)	98.88	99.70	99.11	98.51	98.70	98.98	0.46%

Path B, a two-step process occurs: (i) elimination of malononitrile *via* TS2B (E_a = 11.2 kcal mol^{-1}) generates imine intermediate 7, followed by (ii) intramolecular cyclization *via* TS3B (E_a = 15.6 kcal mol^{-1}) to yield compound **9**. DFT results confirm that Path B is kinetically favored due to its lower activation energy (15.6 kcal mol^{-1} *vs.* 33.0 kcal mol^{-1}), suggesting it likely operates as the dominant route under the reaction conditions. Finally, under heating and aerial oxidation, compound **9** undergoes dehydration to form the fully aromatized target product 10, identified as 2-CPBZ.

3.2.4 The purity and yield of 2-CPBZ. Under the optimized reaction conditions, five replicate experiments were conducted to evaluate the reproducibility of the reaction. As summarized in Table 2, the yield of 2-CPBZ remained consistently above 85% across all replicates, with a relative standard deviation (RSD) below 5%. These results confirm the high reproducibility and robust performance of the synthetic process under the established conditions.

4 Conclusion

In summary, this study establishes a green strategy for the sustainable management of decommissioned explosive tear gas grenades, achieving efficient recovery and value-added conversion of key CS component. Based on the solubility differences of CS and RDX in different solvents, a "methanol extraction–trichloromethane/ethanol stepwise separation" process was developed. The optimal process conditions were determined as heated stirring extraction, solid-to-liquid ratio of 1 : 35, temperature of 55 °C, and time of 30 minutes. Multi-faceted characterization confirmed that the recovered CS is highly consistent with the certified reference. Scale-up experiments and 10-batch reproducibility verification demonstrated a stable CS and RDX recovery rate exceeding 90%, purity over 96%, proving the process's good stability and industrial application potential.

Subsequently, the conversion pathway to 2-CPBZ was systematically investigated using the recovered CS as raw material. The amino protection strategy and activation energy modulation method were fabricated to improve the conversion product yield.

Under the optimal conditions of 70 °C, 3 hours, and OPD-to-CS adduct molar ratio of 1.5 : 1, the average yield of 2-CPBZ reached 86.2%. The product structure was confirmed through spectroscopic analysis, and combined with DFT calculations, a reaction mechanism involving "Michael addition–intramolecular nucleophilic cyclization–oxidative aromatization" was proposed, clarifying the pathway for directional conversion of CS to 2-CPBZ. This integrated approach provides a complete technical pathway for sustainable management of hazardous materials, transforming waste into valuable chemicals while establishing an environmentally sound alternative to conventional disposal methods.

Conflicts of interest

There are no conflicts to declare.

Data availability

All data generated or analyzed during this study are included in this manuscript and its supplementary information (SI).

Supplementary information: data on the solubility curves of CS and RDX, solvent selection, thermogravimetric analysis of RDX, mixing intensity, solvent recycling times, melting point of CS, and the high-value conversion process of CS. See DOI: https://doi.org/10.1039/d6ra01583b.

References

1 M. E. Quiroga-Garza, R. E. Ruiz-Lozano, N. S. Azar, H. M. Mousa, S. Komai, J. L. Sevilla-Llorca and V. L. Perez, *Front. Toxicol.*, 2023, **5**, 118731.
2 R. Sollom and H. G. Atkinson, *Weaponizing Tear Gas: Bahrain's unprecedented use of toxic chemical agents against civilians*, Physicians for Human Rights, Cambridge, MA, 2012.
3 N. Sivathasan, *Emerg. Med. J.*, 2010, **27**, 881–882.
4 J. Akhavan, *The chemistry of explosives 4E*, Royal Society of Chemistry, 2022.
5 N. R. Council, D. o. Engineering, P. Sciences, C. o. Engineering, T. Systems and P. o. Review and E. o. A. C. D. Technologies, *Review and evaluation of alternative chemical disposal technologies*, National Academies Press, 1996.
6 N. R. Council, D. o. Engineering, P. Sciences, C. o. Engineering, T. Systems and C. o. A. C. D. Technologies, *Alternative technologies for the Destruction of Chemical agents and Munitions*, National Academies Press, 1993.
7 N. R. Council, D. o. Engineering, P. Sciences, B. o. A. Science and C. o. Review and E. o. t. A. N.-S. C. M. D. Program, *Evaluation of Alternative Technologies for Disposal of Liquid Wastes from the Explosive Destruction System*, National Academies Press, 2002.
8 Y. C. Yang, J. A. Baker and J. R. Ward, *Chem. Rev.*, 1992, **92**, 1729–1743.
9 T. Kuykendall, Characterization of explosives testing ranges: environmental impacts and remediation considerations, PhD thesis, Selinus University, 2023.
10 C. R. Dempsey and E. T. Oppelt, *Air Waste*, 1993, **43**, 25–73.
11 R. Rathna, S. Varjani and E. Nakkeeran, *J. Environ. Manage.*, 2018, **223**, 797–806.
12 R. Akhundov and E. Hashimov, *Military activity and the environment: The need for a systemic approach to radiological and chemical safety*, ICRC Conference Materials, 2025, pp. 187–197.
13 C. Huang, C. Dong and Z. Tang, *Waste Manage.*, 1993, **13**, 361–377.
14 G. Xi, J. Deng, K. Yang, Z. Cui, T. Luan, C. Hao and S. Zhang, *Energy Environ. Sci.*, 2026, DOI: 10.1039/D5EE06389B.
15 A. Dandia, R. Singh and S. Maheshwari, *Curr. Org. Chem.*, 2014, **18**, 2513–2529.
16 A. F. Darweesh, N. A. Abd El-Fatah, I. A. Abdelhamid, A. H. Elwahy and M. E. Salem, *Synth. Commun.*, 2020, **50**, 2531–2544.
17 R. G. Menezes, S. A. Hussain, M. A. M. Rameez, M. A. Kharoshah, M. Madadin, N. Anwar and S. Senthilkumaran, *Med.-Leg. J.*, 2016, **84**, 22–25.
18 G. Shrivastav, T. Prava Jyoti, S. Chandel and R. Singh, *Sep. Purif. Rev.*, 2025, **54**, 241–257.
19 V. S. Kislik, *Solvent extraction: classical and novel approaches*, Elsevier, 2011.
20 M. A. Butturi, A. Neri, F. Mercalli and R. Gamberini, *Environments*, 2025, **12**, 82.
21 S. Dutta, *ChemPlusChem*, 2025, **90**, e202400568.
22 P. Yadav, S. Berry and A. Bhalla, *Synthesis*, 2025, **57**, 251–274.
23 O. O. Ajani, D. V. Aderohunmu, C. O. Ikpo, A. E. Adedapo and I. O. Olanrewaju, *Arch. Pharm.*, 2016, **349**, 475–506.
24 K. Keerthi Krishnan, S. M. Ujwaldev, S. Saranya, G. Anilkumar and M. Beller, *Adv. Synth. Catal.*, 2019, **361**, 382–404.
25 M. T. Jafari-Chermahini and H. Tavakol, *Res. Chem. Intermed.*, 2023, **49**(9), 4065–4086.
26 B. Dik, D. Coşkun, E. Bahçivan and K. Üney, *Turk. J. Med. Sci.*, 2021, **51**, 1579–1586.
27 M. Marinescu, *Antibiotics*, 2023, **12**, 1220.
28 S. Yadav, B. Narasimhan, S. M. Lim, K. Ramasamy, M. Vasudevan, S. A. A. Shah and A. Mathur, *Egypt. J. Basic Appl. Sci.*, 2018, **5**, 100–109.
29 L. S. Feng, W. Q. Su, J. B. Cheng, T. Xiao, H. Z. Li, D. A. Chen and Z. L. Zhang, *Arch. Pharm.*, 2022, **355**, 2200051.
30 S. Venugopal, B. Kaur, A. Verma, P. Wadhwa, M. Magan, S. Hudda and V. Kakoty, *Chem. Biol. Drug Des.*, 2023, **102**, 357–376.
31 K. Haider and M. S. Yar, *Benzimidazole*, 2022.
32 M. Nardi, N. C. H. Cano, S. Simeonov, R. Bence, A. Kurutos, R. Scarpelli, D. Wunderlin and A. Procopio, *Catalysts*, 2023, **13**, 392.
33 P. Rajguru, P. Bora, C. Bhuyan and S. Hazarika, *Mater. Adv.*, 2026, **7**, 682–714.
34 S. Johari, M. Rafie Johan and N. Ghaffari Khaligh, *Curr. Org. Synth.*, 2024, **21**, 704–716.
35 V. Gheorghe, C. G. Gheorghe, D. R. Popovici, S. Mihai, C. Calin, E. E. Sarbu, R. Doukeh, N. Grigoriu, C. N. Toader and C. Epure, *Toxics*, 2023, **11**, 672.
36 V. Gheorghe, C. G. Gheorghe, D. R. Popovici, S. Mihai, D. R. Elena and R. Șomoghi, *Modification of Oxygen Production of Algal Cells in the Presence of O-chlorobenzylidene Malononitrile, Biodegradation in the Eco-Friendly Way*, 2023, DOI: 10.20944/preprints202311.0622.v1.
37 I. G. Binev, Y. I. Binev and I. N. Juchnovski, *Spectrosc. Lett.*, 2002, **35**, 285–291.
38 F. F. Fleming and Q. Wang, *Chem. Rev.*, 2003, **103**, 2035–2078.
39 Z. Hu, F. Zhang, Y. Mao, C. Li, L. Chen, F. Sun, D. Liu and Y. Gu, *Waste Biomass Valorization*, 2024, **15**, 4785–4791.
40 H. A. Elagab, *Synthesis*, 2016, **3**, 4.
41 V. N. Mahire and P. P. Mahulikar, *Chin. Chem. Lett.*, 2015, **26**, 983–987.
42 E. Pham, T. Thi, H. Hong, B. Thi, L. Vong and T. Vu, *RSC Adv.*, 2023, **13**, 399–420.
43 F. Odame, J. Krause, E. C. Hosten, R. Betz, K. Lobb, Z. R. Tshentu and C. L. Frost, *Bull. Chem. Soc. Ethiop.*, 2018, **32**, 271–284.